by A. Gago, J. Proença, J. Cardoso, V. Cóias, and R. Paula

SEISMIC STRENGTHENING OF STONE MASONRY WALLS WITH GLASS FIBER REINFORCED POLYMER STRIPS AND MECHANICAL ANCHORAGES

Traditional stone masonry is a composite structural material consisting of irregular stone units aggregated by lime mortar. Stone masonry walls are adequate for predominantly compressive stress states, such as those due to vertical loads, but are particularly prone to failure when subjected to out-of-plane (lateral) loads caused by earthquakes. Adequate strengthening methodologies addressing this limited lateral deformation capability of load-bearing stone masonry walls are therefore of the utmost importance in high-seismic hazard regions. With the scientific support of ICIST, STAP SA has developed a proprietary seismic-strengthening technique for traditional masonry structures, consisting in externally bonded glass fiber reinforced polymer (GFRP) strips and mechanical anchorages. This methodology—developed to enhance the out-of-plane behavior of stone masonry walls, improving the bending and shear strength, as well as ductility and energy dissipation capacity—was recently tested and improved by ICIST through an extensive experimental program. This paper presents a comprehensive description of the test program, including the innovative test setup and results. Moreover, a strengthening design procedure for out-of-plane behavior of masonry walls, developed based on experimental evidence, is also presented.

DESCRIPTION OF THE STRENGTHENING SYSTEM

The proposed strengthening technique for traditional load-bearing stone masonry walls (50–80-cm thick) consists of the application of GFRP strips on one or, preferably, on both wall faces, connected to the masonry substrate through epoxy resin and mechanical anchorages.

The anchorage system prevents slip and debonding of the GFRP laminate from the masonry substrate and increases the wall lateral confinement and, therefore, its compressive strength. As a result, the reinforcement system has a double effect on masonry walls: increasing bending strength and ductility for out-of-plane loads, and improving shear and compressive strength for in-plane loads.

Figure 1 shows schematic views of a strengthening proposal, using the described technique, on a typical 19th century Lisbon building, and Fig. 2 depicts a typical detail. GFRP strips (10–20-cm wide), assembled and impregnated with epoxy resin, are applied on the wall face in two layers, connected to the masonry substrate by epoxy resin and anchorages. The anchorages, metallic or composite tie rods, are placed on the wall face in drills over pre-existent or deliberately created grooves (stone joints or chiselled recesses, respectively). The first (inner) layer of GFRP is directly applied onto the masonry wall, adjusting to the shape of the groove, after which the groove is completely filled with epoxy mortar, and the second (outer) layer is stretched over the resulting flat surface. The anchoring plates, metallic or composite, are then attached to the tie rods, thus compressing the grooves and the underlying masonry substrate. The working principle of the anchorage is as follows: when the masonry wall is subjected to flexure, the inner layer of the tensioned GFRP strip tends to straighten up, pushing the anchoring plate which is prevented from going outward by the tie rod, thus blocking the slippage of the GFRP.

Compared with the traditional strengthening methods for masonry walls,[3,4,5] this methodology presents some advantages, such as lower intrusiveness, negligible increase in mass and wall thickness, dry nature of the method (without hydraulic mortars), ease of application, and non-corrosiveness of the reinforcement material.

EXPERIMENTAL PROGRAM

The flexural behavior of stone masonry walls strengthened with externally bonded and anchored GFRP laminates is highly influenced by the effectiveness of the GFRP-masonry substrate interface. Consequently, the assessment of the most influential bonding factors and their effects on an out-of-plane design model for strengthened masonry walls was the main objective of the experimental program. A total number of 29 masonry specimens were tested in this program. These specimens were cast with a special mortar trying to reproduce the compressive strength, elasticity modulus, and bonding characteristics of traditional stone masonry walls.

Materials

The experimental program started with the mechanical characterization of mortar and GFRP laminates. Compressive tests on mortar-masonry cubic specimens (150-mm side), performed according to the Portuguese National Standard LNEC E226,[6] indicated an average compressive strength of 1.30 MPa. Tensile tests were performed on six GFRP laminates specimens (three single-layer [SL] and three double-layer [DL]), and the results are summarized in Table 1. Tests on GFRP laminates were performed according to the following ISO standards: 527-1,[7] 527-4,[8] and 527-5.[9]

When the mechanical characteristics are computed based solely on the fiber cross section two apparently contradictory effects arise: the elastic modulus is about double of that of

A. Gago (gago@civil.ist.utl.pt) and J. Proença are assistant professors and J. Cardoso is a researcher affiliated with the Department of Civil Engineering and Architecture, Technical University of Lisbon, Instituto Superior Tecnico, ICIST, Lisbon, Portugal. V. Cóias and R. Paula are civil engineers affiliated with the STAP SA - Reparação, Consolidação e Modificação de Estruturas, SA, Portugal.

doi: 10.1111/j.1747-1567.2009.00544.x

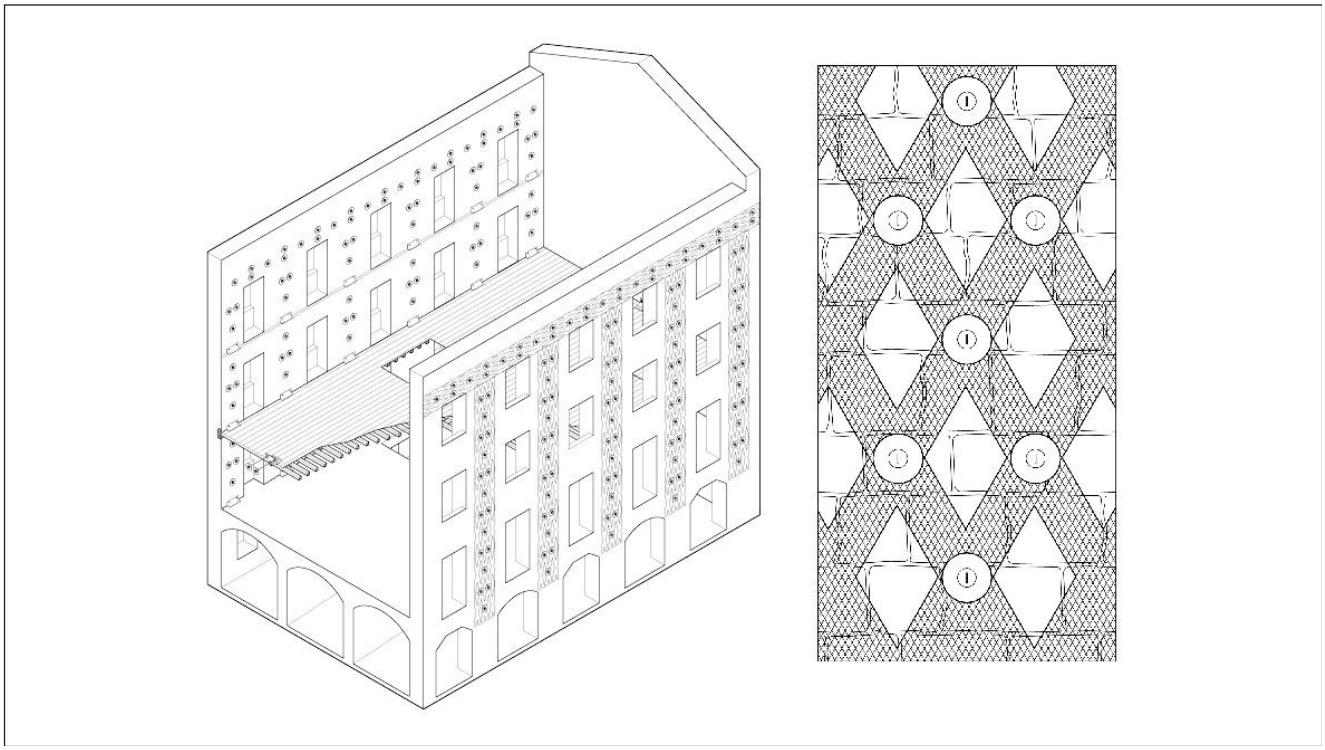

Fig. 1: View of a masonry building reinforced with GFPR strips and anchorages.[1] Note: although less effective for out-of-plane bending, strips are depicted oriented along oblique directions, with increased benefits for in-plane shear

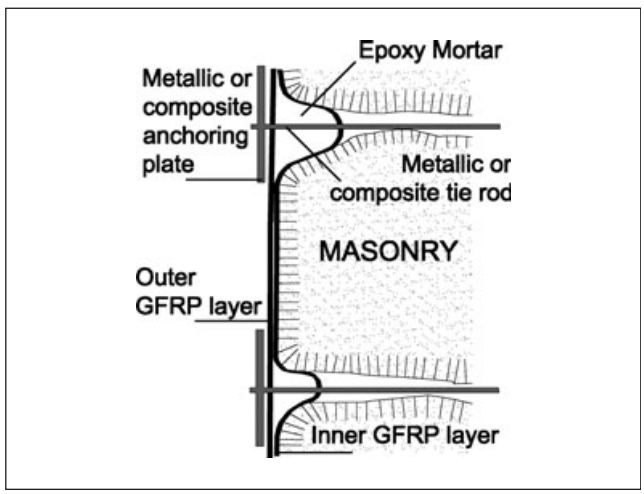

Fig. 2: Detail of the GFRP double-layer reinforcement solution and of the anchorage system[2]

the manufacturer data for virgin filaments ($E_f = 65$ GPa), whereas the maximum strength is about half of the manufacturer value ($\sigma_{fu} = 3$ GPa). The first effect can be explained by the fact that the contribution of the epoxy matrix is neglected, leading to an over estimation of the fiber stress. Despite that, the detrimental consequences due to the inclusion of the fiber in the matrix are such that the maximum fiber stress, computed in the same way, falls significantly below the manufacturer specifications for filaments (second effect). All these conclusions are in line with either the well-known "rule of mixtures"[10] or the manufacturer design recommendations[11] (consideration of the fiber cross section and cumulative reduction of the strength by a design factor of 1.5–1.8).

Test Configuration

Different setups have been used in the past to study the stress distribution and deformation along the bonded length[12,13] (Fig. 3). The test setup adopted for the present study resulted from modifications carried out on the "beam test" configuration, which originally implies the use of two blocks per test. One of these modifications, aiming at the reduction of the total number of masonry blocks, consisted in the use of a dummy steel block, the same in all tests, leading to a single mortar block being damaged at each test (Fig. 4). Another modification consisted in the location of the compression hinge at mid-height of the specimen cross section (20×30 cm^2, length 130 cm). Except for a rigid body rotation, the setup is similar to the "single-shear" configuration, with a state of pure tension in GFRP. Figure 5 shows the test setup and the steel frame assembled for the present experimental programme.

Test Loading

Testing procedure was as follows: (1) release of the provisional tie system, activating the fiber tensile stresses

Table 1—Results from tensile tests on GFRP laminates

SPECIMEN	FIBER CROSS SECTION (mm^2)	COMPOSITE CROSS SECTION (mm^2)	ELASTIC MODULUS (GPa) BASED ON		TENSILE STRENGTH (MPa) BASED ON	
			FIBER CROSS SECTION	COMPOSITE CROSS SECTION	FIBER CROSS SECTION	COMPOSITE CROSS SECTION
SL1	7.45	74.25	117.45	11.78	1630.87	163.64
SL2	7.45	80.00	116.78	10.88	1759.73	163.88
SL3	7.45	85.00	124.83	10.94	1761.07	154.35
Average			119.69	11.20	1717.23	160.62
DL 1	14.90	125.00	134.56	16.04	1275.84	152.08
DL 2	14.90	126.25	122.15	14.42	1357.05	160.16
DL 3	14.90	123.25	107.05	12.94	1448.32	175.09
Average			121.25	14.47	1360.40	162.44

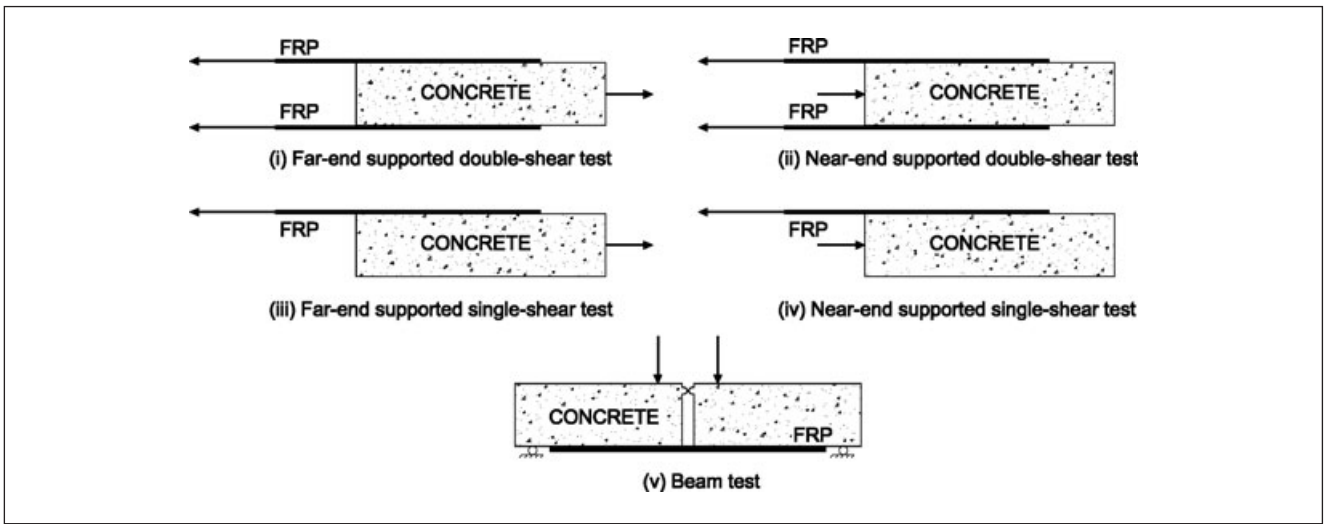

Fig. 3: Configurations for bond tests[13]

to balance the self-weight of the blocks; (2) stepped loading, monotonic or cyclic (repeated with increasing force amplitude), through the hydraulic jack and the distribution beam.

Masonry Specimens

Masonry specimens were reinforced with 10-cm-wide GFRP strips and anchorages, following the described methodology. A special GFRP strip-anchoring device on the dummy block was conceived for the testing program (Fig. 6). The anchorage procedure consisted in folding the composite strip (before hardening) around two steel plates and clamping this set with adjustable bolts.

Considering that the existence and detailing of anchorages is a distinctive feature of the strengthening technique, a total number of 29 reinforced specimens were tested, with different numbers of anchorages (1 or 2) and spacing (25, 50, or 75 cm). Masonry specimens were divided into six general series, one for each anchorage spacing/number combination (Table 2). The identification of each specimen was as follows: a specimen with "n" anchorages, spaced "s" centimeters, is designated by Ms-n-120, where the number 120 indicates the fiber-bonded length (in cm). Each series generally comprised four specimens, of which three were subjected to monotonic loading (suffix M) and the fourth was subjected to cyclic, repeated loading (suffix C). The loading history was as described: monotonic tests—increasing load with 1-kN increments until collapse; cyclic tests—repeated cycles with increasing amplitude starting and ending at 1 kN 2 kN (one cycle), 3 kN (one cycle), 4 kN (three cycles), 7 kN (three cycles), 10 kN (three cycles), 13 kN (three cycles),. . ., until collapse. One control specimen, without anchorages, was further tested to assess the beneficial effects of the anchorages. As shown in Fig. 5, the test instrumentation comprised a load cell, six displacement transducers (to measure the block rotation), and several strain gages on the GFRP laminate (one in the beam mid-span, one for each anchorage position, and one for each of the segments between anchorages).

Experimental Tests

The experimental program started with a monotonic loading test on the M75-2-120 (M1) specimen, reinforced with a

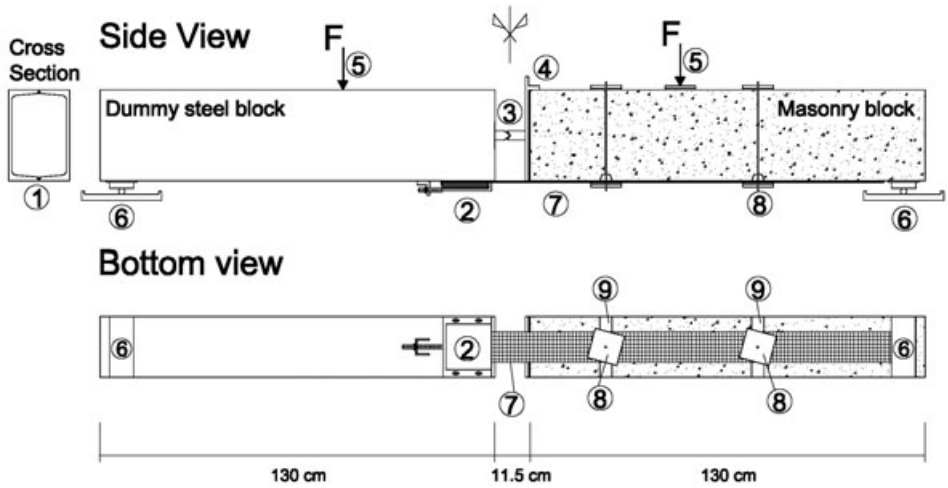

1. 2 UNP 300; 2. fiber anchoring device; 3. compression hinge; 4. steel plate; 5. applied force; 6. vertical support; 7. composite GFRP; 8. anchorage or confinement connector (steel plate + steel tie rod); 9. groove.

Fig. 4: Test configuration (side and bottom views, masonry block on the right)

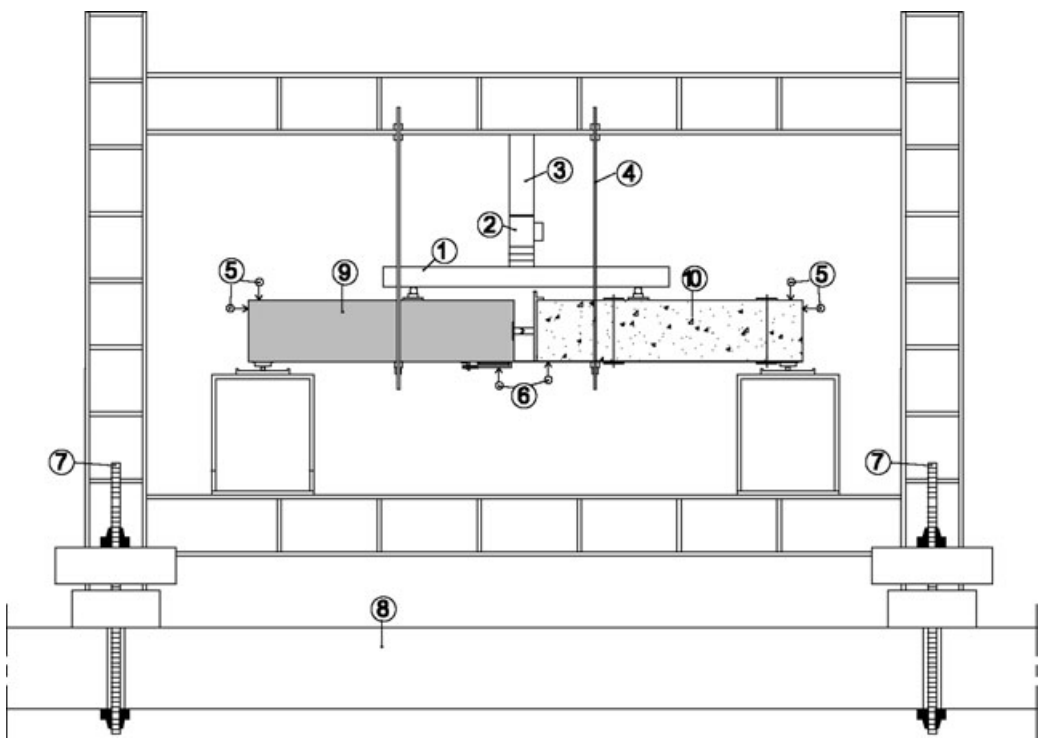

1. Load distribution beam; 2. load cell; 3. hydraulic jack; 4. provisional tie system; 5/6. displacement transducers; 7. dywidag bar; 8. stiff floor; 9. dummy steel block; 10. masonry block

Fig. 5: Test setup (side view)

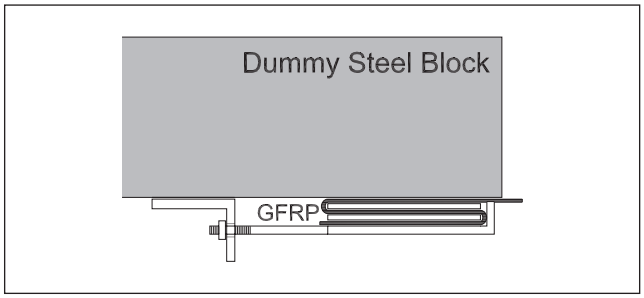

Fig. 6: Detail of fiber anchoring device in steel block

bidirectional glass fabric with a longitudinal fiber cross section of 13.00 mm^2 (50/50 distribution with a total weight per layer of 350 g/m^2). In this test, failure occurred by tensile fracture of the GFRP strip before the anchorage closest to the compression hinge (T failure, Fig. 7a), which showed negligible damage effects. To instigate the participation of the anchorages, the remaining specimens were strengthened with a more resistant uni-directional glass fabric (with a longitudinal fiber cross section of 29.80 mm^2, 90/10 distribution with a total weight per layer of 440 g/m^2). In the remaining tests of the series M75-2-120 (M2, M3, M4, and C1), the maximum developed stress in the GFRP (uni-directional fabric) increased, and failure occurred due to premature cutting of the laminate on contact with the sharp edges of the anchoring device (N_1 failure, Fig. 7b). To avoid this premature failure, the edges of the anchoring device were smoothed and an additional GFRP layer was placed in the strip within this device. None of these changes had any influence on the bonding behavior along the reinforced masonry block. The succeeding test stage corresponded to two M25-2-50 specimens, M1 and M2, with a reduced (50 cm) strip length, which led to a sudden discontinuity in terms of the bending strength of the masonry block. In these two specimens, failure, as expected, was due to premature laminate debonding, a phenomenon that started from the extremity opposed to that of the compression hinge (D* failure, Fig. 8a). In the remaining test specimens, the GFRP laminate was extended to near the support (120 cm long), where the bending moments are negligible. In the following tests, M25-2-120 (M3, M4, M5, C1, and C2), failure predominantly resulted from laminate cutting on first innermost anchoring plate (N_2 failure, Fig. 8b). This failure mode corresponded to a better use of the GFRP high-strength fabric, resulting from full anchorage effect. Failure of M50-1-120 and M75-1-120 specimens, reinforced with only one anchorage, occurred due to GFRP laminate debonding along the full length and damage of the anchorage system (D failure, Fig. 9a). In series M50-2-120 and M75-2-120, reinforced with two anchorages, failure occurred respectively due to laminate cutting on the first innermost anchoring plate (N_2 failure), and due to laminate cutting on contact with the anchoring device (N_1 failure). Specimens of series M25-1-120 collapsed by crushing of the compressed masonry strut, which developed between the anchorage and the compression hinge (C failure, Fig. 9b). Finally, specimen M120, reinforced with no anchorages, collapsed by laminate debonding during the initial stage of the test, when releasing the provisional tie system (bond strength was insufficient to balance the self-weight of the blocks).

Tests showed that increased spacing of the anchorages will give rise to debonding failure, while decreased spacing may lead to collapse due to masonry crushing. Anchorage spacing similar to the traditional masonry wall thickness (50–80 cm) seems to be appropriate, leading to less fragile failure modes. Finally, tests showed the need for anchoring the GFRP laminate ends or to extend the GFRP laminate to zones where bending moments are negligible, thus avoiding premature debonding.

Test Results

Table 3 summarizes the most relevant results of the experimental program. The first general conclusion is that the strengthening technique is extremely effective, allowing high tensile stresses to be developed in the GFRP strips, which, in turn, led to a wide variety of premature failure

Table 2—Specimen identification and characteristics

SPACING BETWEEN ANCHORAGES	NUMBER OF ANCHORAGES	SERIES NAME	LOADING TYPE	NUMBER TESTS	TEST NAME
25 cm	1	M25-1	Monotonic	3	M25-1-120 (M1 to M3)
			Cyclic	1	M25-1-120 (C1)
	2	M25-2	Monotonic	5	M25-2-120 (M1 to M5)
			Cyclic	2	M25-2-120 (C1 to C2)
50 cm	1	M50-1	Monotonic	3	M50-1-120 (M1 to M3)
			Cyclic	1	M50-1-120 (C1)
	2	M50-2	Monotonic	3	M50-2-120 (M1 to M3)
			Cyclic	1	M50-2-120 (C1)
75 cm	1	M75-1	Monotonic	3	M75-1-120 (M1 to M3)
			Cyclic	1	M75-1-120 (C1)
	2	M75-2	Monotonic	4	M75-2-120 (M1 to M4)
			Cyclic	1	M75-2-120 (C1)
	0	M120	Monotonic	1	M120 (M1)

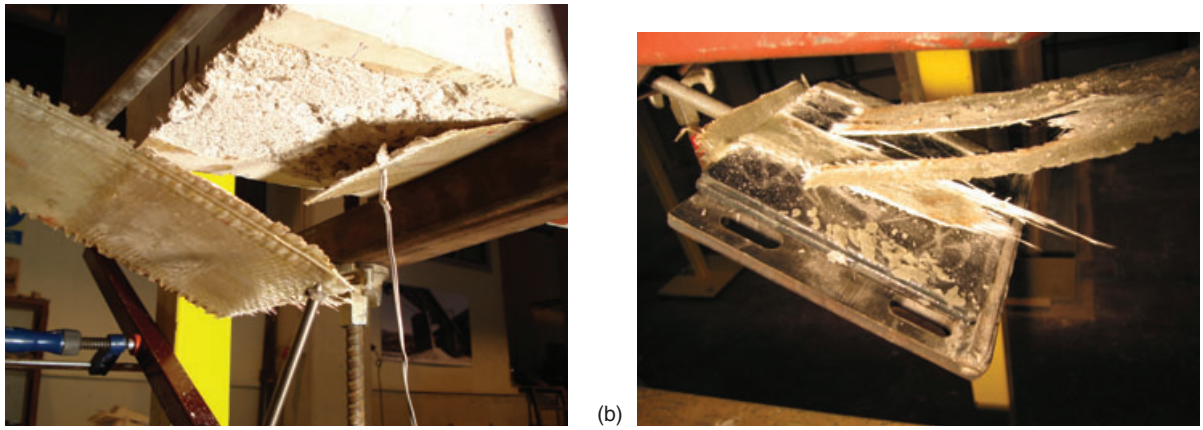

Fig. 7: (a) GFRP tensile fracture—test M75-2-120 M1 (T failure); (b) GFRP cut due to stress concentration in the edges of the anchoring device (N_1 failure)

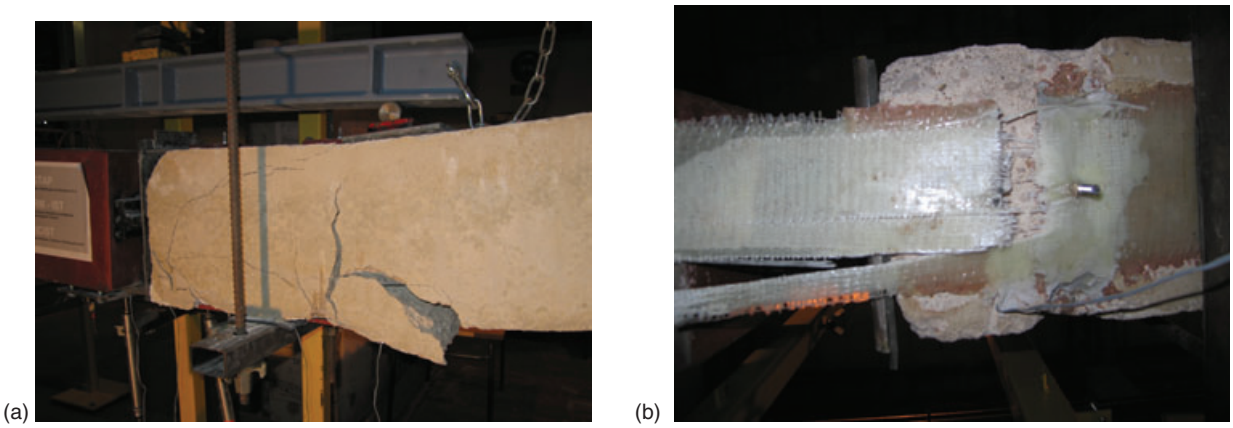

Fig. 8: (a) GFRP debonding starting from the laminate end (D* failure); (b) GFRP cut on the first innermost anchoring plate (view after dismounting the anchorage system) (N_2 failure)

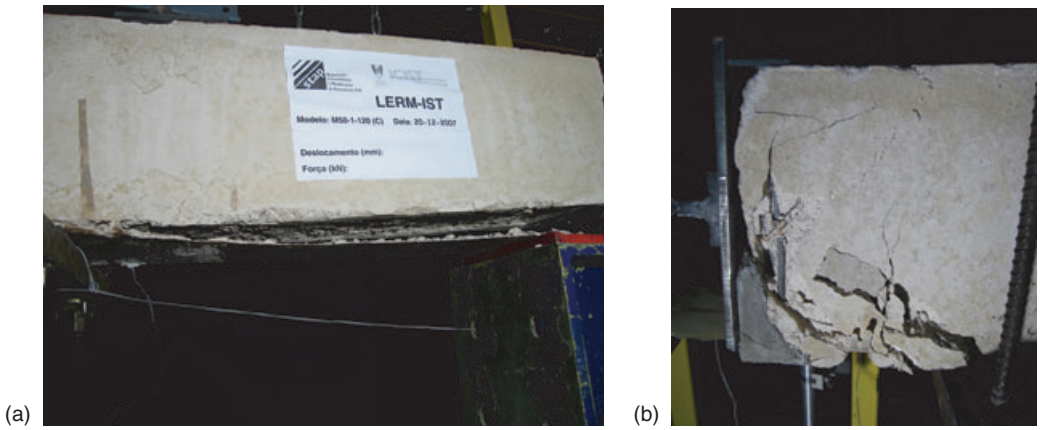

Fig. 9: (a) GFRP debonding after the anchorage (D failure); (b) Masonry crushing (C failure)

modes in the tests. Tensile stresses in the order of 1 GPa can be computed in the GFRP if the epoxy resin area is neglected in the calculations. Results corresponding to premature failure modes (N_1, D* failure) are shaded as well as those in which failure occurred due to masonry crushing (C). Both of these failure modes can be regarded as collateral effects of the test setup. Maximum GFRP strain at collapse (measured by strain gages placed on the laminate in the beam mid-span) generally exceeded 8% in all specimens that presented realistic failure modes. Because all single anchorage specimens collapsed due to premature failure or collateral test setup effects, no conclusions

Table 3—Experimental results

SERIES	LOADING TYPE	NUMBER OF ANCHORAGES	SPACING BETWEEN ANCHORAGES (cm)	BONDED FIBER LENGTH (cm)	FIBER CROSS SECTION A_f (mm^2)	FAILURE MODE	MAX. GFRP FORCE F_u (kN)	MAX. GFRP STRAIN ε_u (‰)
M25-1	M1	1		120	29.80	C	26.04	6.08
	M2				29.80	C	24.00	5.43
	M3				29.80	C	26.00	6.83
	C1				29.80	C	38.93	12.94
M25-2	M1	2	25	50	29.80	D*	31.78	7.79
	M2				29.80	D*	28.24	6.76
	M3			120	29.80	N_2	31.86	7.70
	M4				29.80	N_2	38.13	13.74
	M5				29.80	N_1	34.34	13.89
	C1				29.80	N_1	34.27	11.08
	C2				29.80	N_2	33.26	14.61
M50-1	M1	1		120	29.80	N_1	32.37	9.37
	M2				29.80	D	32.93	9.92
	M3				29.80	D	28.28	8.33
	C1				29.80	D	26.06	8.37
M50-2	M1	2	50	120	29.80	C/A	35.78	12.38
	M2				29.80	N_2	38.16	11.58
	M3				29.80	N_2	40.73	12.03
	C1				29.80	N_2	36.04	13.34
M75-1	M1	1		120	29.80	D	35.83	8.97
	M2				29.80	D	28.33	9.28
	M3				29.80	D	28.40	8.85
	C1				29.80	D	30.70	9.86
M75-2	M1	2	75	120	13.00	T	21.96	11.83
	M2				29.80	N_1	36.09	8.47
	M3				29.80	N_1	39.95	7.75
	M4				29.80	N_1	25.90	12.49
	C1				29.80	N_1	35.70	11.83
M120	M1	0	∞	120	0	D	8.90	

D, GFRP debonding; D*, GFRP debonding at laminate end; T, GFRP tensile fracture; N, GFRP cut fracture on the anchoring device (N_1) or on the anchorage system (N_2); C, masonry crushing; A, anchorage failure.

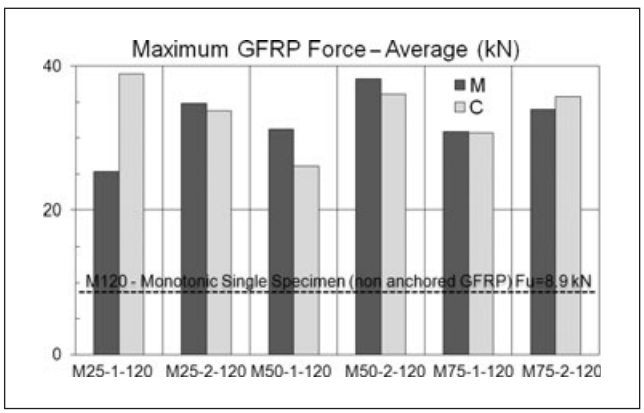

Fig. 10: Strength increase compared to the traditional reinforcement solution, without anchorages

regarding the influence of the number of anchorages can be derived. Nonetheless, double anchorage specimens generally presented higher levels of deformation capacity, due to stress redistribution between the innermost and outermost anchorages. Maximum composite force showed that no significant dependency on the anchorage spacing for the spacing range considered. Contrary to what could be expected, there was no consistent decrease in strength in specimens subjected to cyclic load history. Figure 10 summarizes the maximum composite force, normalized with respect to that of the specimen reinforced without anchorages. Data are presented grouping all tests according to the number and spacing of anchorages and loading pattern. This figure clearly shows a significant increase in strength developed in specimens with anchorages, thus proving the effectiveness of this anchoring system in taking maximum advantage of the GFRP strength.

DESIGN MODEL FOR OUT-OF-PLANE BEHAVIOR

The effectiveness of the strengthening system was further studied through the development of a calculation model for the design of the strengthened walls when subjected to combined compression and out-of-plane flexure. This model is based on the following assumptions[14,15,16]:

- Bernoulli's hypothesis (plane sections remain plane);
- Full adherence hypothesis (same strain in GFRP and in the underlying masonry);
- No tensile and compression strength, respectively, for masonry and GFRP materials;
- The stress–strain constitutive law for the composite is based on the GFRP material alone, neglecting the mechanical contribution of the epoxy resin (due to fact that there is no strict control of the mixture process and its final thickness);
- Constitutive laws: parabolic for compressed masonry and linear elastic (up to failure) for GFRP reinforcement subjected to tension.

Furthermore, the material constitutive laws were characterized by the following values: ultimate tensile strain of 8% for GFRP reinforcement; crushing strain of 2% (full compression) or 3.5% (compression and bending) and

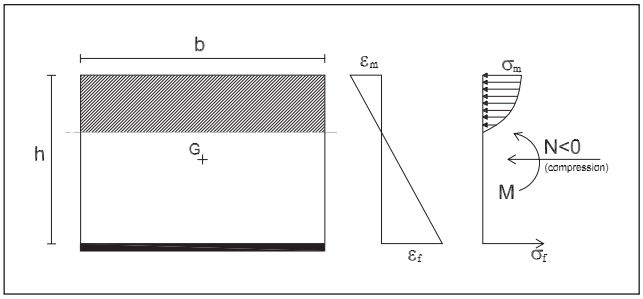

Fig. 11: Computation of the out-of-plane bending resistant moment: strain and stress diagrams (ε_m and σ_m represent the maximum compressive strain and stress on masonry and ε_f and σ_f the GFRP fiber tensile strain and stress)

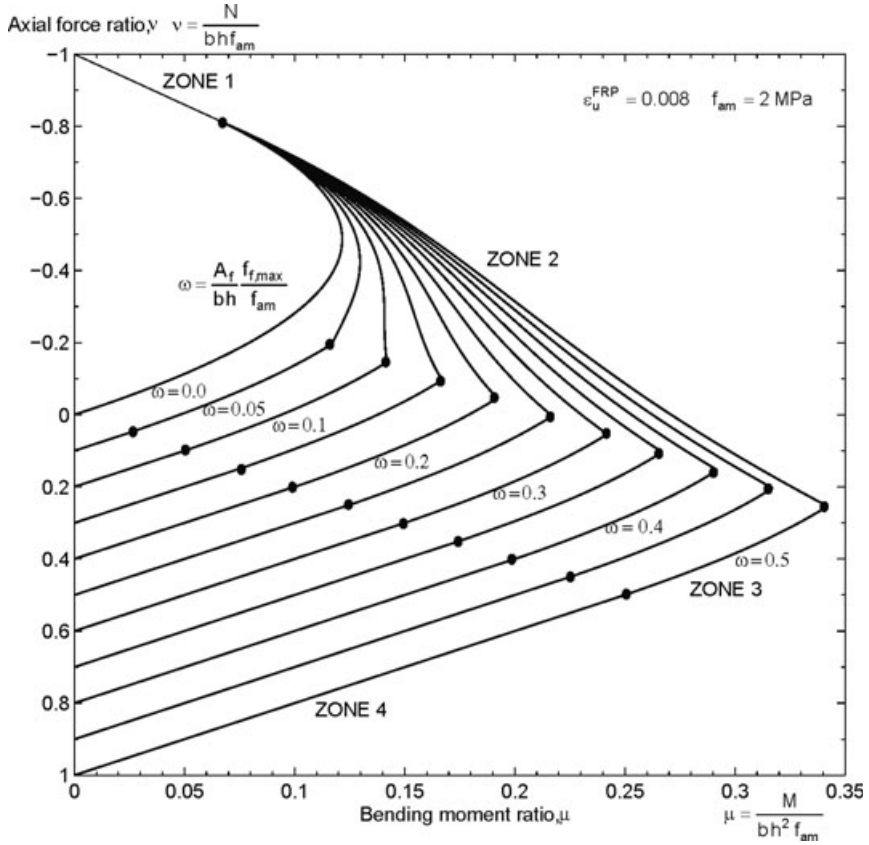

Failure Mode-Masonry crushing: Zone 1. fully compressed cross section; Zone 2. partially compressed cross section;
Failure Mode-GFRP tensile fracture or debonding: Zone 3. partially compressed cross section; Zone 4. fully tensioned cross section.

Fig. 12: Typical design curve for masonry walls reinforced with the proposed technique

maximum strength of 2 MPa, for compressed masonry. Figure 11 represents the general stress and strain cross sectional (bxh) distribution for a strengthened wall subjected to axial compression (N) and out-of-plane flexure (M).

For each mechanical reinforcement ratio value (ω) and considering all possible limit situations (masonry crushing and GFRP tensile failure), the ultimate design bending moment and axial force combinations can be computed, as depicted in Fig. 12. Figure 12 illustrates that, with the exception of highly compressed walls (axial force ratio $\nu < -0.5$), strengthening results in a significant increase in the bending capacity of the wall.

CONCLUSIONS

This paper presents a strengthening technique for traditional load-bearing stone masonry walls. The technique consists in the application of GFRP strips on masonry wall faces, bonded to the substrate and further connected to it through mechanical anchorages. The effectiveness of this technique is highly dependent on the capability of developing high stresses on the composite reinforcement, which, in turn, depends on bonding and anchorage effectiveness. For this reason, an extensive experimental program devoted to the study of interface bonding was conducted. An innovative test setup was developed, consisting of modifications carried out on the "beam test" configuration, with the use of a dummy steel block, thus leading to a reduction of the number of manufactured masonry blocks. A total number of 29 specimens were tested, varying, amongst other things, the number and spacing of anchorages. As a general conclusion of the experimental program, it can be stated that the existence of anchorages proves to be highly beneficial in increasing the strength and deformation capacity of strengthened masonry walls. Tests have shown that the strengthening technique is extremely effective, leading to high tensile stresses in the GFRP strips, which, in turn, led to premature failure modes in some of the tests. Specimens with multiple anchorages have shown higher deformation capacity than those with single anchorage. Maximum composite force showed no significant dependency on the anchorage spacing and a consistent decrease in strength in specimens subjected to cyclic load history was not identified. Increasing anchorage spacing may lead to debonding failure, whereas decreasing spacing leads to an increase in cost and workmanship. An intermediate spacing—in the order of magnitude of the wall thickness—is recommended. A calculation model for the design of strengthened walls when subjected to combined compression and out-of-plane flexure is also presented, and illustrated with some typical results. These results clearly show the effectiveness of the strengthening system, with a significant strength increase in moderately compressed walls.

References

1. Cóias e Silva, V., "Preserving Baixa Pombalina Trough Low Intrusive Seismic Rehabilitation Methods. The COMREHAB Project," ESTUA, SPES, and Martins, C. (eds), *4º Encontro Nacional Sobre Sismologia e Engenharia Sísmica*, Faro, Portugal (1999).
2. Cardoso, J., Proença, J., Gago, A., Cóias, V., and Paula, R., "Development of a Reduced Intrusiveness Seismic Strengthening Technique in Traditional Masonry Walls through GFRP Strips and Anchorages. Bonding Tests and Design Model," *International Seminar on Seismic Risk and Rehabilitation of Stone Masonry Housing*, S. Miguel, Portugal; July 9–13, 2008.
3. ACI, "Report on Fiber-Reinforced Polymer (FRP). Reinforcement for Concrete Structures," ACI Committee 440: ACI 440XR (2006).
4. CNR-DT, "Guide for the Design and Construction of Externally Bonded FRP Systems for Strengthening Existing Structures: materials, RC and PC Structures, Masonry Structures," CNR-DT 200/2004, Rome, Italy (2004).
5. Jifu, L., Ming, L., and Yupu, S., Experimental Investigation on Flexural Performance of Masonry Walls Reinforced with GFRP, *Journal of Wuhan University of Technology-Materials Science Edition* **22**(1):82–84 (2007).
6. LNEC, E226 Standard, *Betão. Ensaio de Compressão* (in Portuguese), Laboratório Nacional de Engenharia Civil, Lisbon, Portugal (1993).
7. ISO, Standard 527-1:1993, *Plastics - Determination of Tensile Properties - Part 1: General Principles* (1993).
8. ISO, Standard 527-4:1997, *Plastics - Determination of Tensile Properties - Part 4: Test Conditions Isotropic and Orthotropic Fibre-reinforced Plastic Composites* (1997).
9. ISO, Standard 527-5:1997, *Plastics - Determination of Tensile Properties - Part 5: Test Conditions for Unidirectional Fibre-reinforced Plastic Composites* (1997).
10. FIB, "Externally Bonded FRP Reinforcement for RC Structures," *Bulletin N. 14, Fédération Internationale de Béton*, Lausanne, Switzerland (2001).
11. S&P, *Design Guide Line for S&P FRP Systems*, S&P Clever Reinforcement Company, Brunnen, Switzerland (2001).
12. Kiss, R.M., Jai, J., Kollar, L.P., and Krawinkler, H., "FRP Strengthened Masonry Beams. Part I –Model," *Journal of Composite Materials* **36**(5):521–536 (2002).
13. Chen, J., Yang, Z., and Holt, G., "FRP or Steel Plate to Concrete Bonded Joints: effects of Test Methods on Experimental Bond Strength," *Steel and Composites Structures* **1**(2):231–244 (2001).
14. Yao, J., Teng, J.G., and Chen, J.F., "Experimental Study on FRP-to-Concrete Bonded Joints," *Journal of Composites: Part B: Engineering* **36:**99–113 (2005).
15. Kiss, R.M., Jai, J., Kollar, L.P., and Krawinkler, H., "Masonry Strengthened with FRP Subjected to Combined Bending and Compression, Part II –Test Results and Model Predictions," *Journal of Composite Materials* **36**(09):1049–1063 (2002).
16. Tumialan, J., Galati, N., and Nanni, A., "Fiber-Reinforced Polymer Strengthening of Unreinforced Masonry Walls Subject to Out-of-Plane Loads," *ACI Structural Journal* **100**(3):321–329 (2003).■